Multiple scattering of light in a system of interacting Brownian particles

1980 J. Phys. A: Math. Gen. 13 2155

(http://iopscience.iop.org/0305-4470/13/6/037)

J. Phys. A: Math. Gen. **13** (1980) 2155–2170. Printed in Great Britain

Multiple scattering of light in a system of interacting Brownian particles

F Grüner and W Lehmann

Fakultät für Physik, Universität Konstanz, Bücklestrasse 13, 7750 Konstanz, FRG

Received 22 July 1979, in final form 6 November 1979

Abstract. The multiple scattered light from a system of interacting Brownian particles, both polarised and depolarised, is studied experimentally by means of correlation spectroscopy. Results obtained in a range of medium to high particle concentration are reported. The first cumulant has different values for the polarised and depolarised components. For two different concentrations the angular dependence of the multiple scattering is measured. Due to the particle interaction, the decay times show a remarkable angular dependence. The results are discussed on the basis of recent theories. A method is proposed to correct the correlation functions of parallel polarised scattered light for multiple scattering which will be applicable for small spherical scatters.

1. Introduction

In the last few years photon correlation spectroscopy has become a very common method for studying the temporal behaviour of fluctuations such as the diffusion of macromolecules in solution (Berne and Pecora 1976).

For very dilute systems the results are well established both theoretically and experimentally. For a system of spherical particles in the limit of infinite dilution, the normalised field correlation function $g^1(\tau)$ has the form of a single exponential with a decay constant given by $-D_0K^2$ (Berne and Pecora 1976), where K is the momentum transfer and D_0 is the free particle diffusion constant given by the well-known Einstein relation $D_0 = kT/6\pi\eta r_H$, where r_H is the so called hydrodynamic radius.

The assumption of infinite dilution, however, is not always fulfilled, especially if one wants to study highly concentrated interacting systems, such as real biological systems. With increasing concentration, the appearance of multiple scattering may heavily distort the correlation function and it is clearly necessary to correct for multiple scattering in order to obtain reliable results. To make reasonable corrections, one has to know how the multiple scattering shows up in the correlation function. Therefore in this paper we investigate experimentally the multiple scattering, both depolarised and polarised, in a concentration range from medium to high concentrations with interactions between particles present. We show the influence of particle interactions on the angular dependence of the multiple scattering for two different examples of moderate and high concentrations respectively.

From the obtained results a method is proposed, applicable to small spherical scatters, to correct the polarised scattering, which is a mixture of singly and multiply scattered light, for the multiple scattering.

0305-4470/80/062155+16$01.50

2. Experimental

The samples used for the experiments were suspensions of spherical polystyrene particles (radius $0{\cdot}045 \pm 0{\cdot}002$ μ and $0{\cdot}055 \pm 0{\cdot}001$ μ respectively) supplied by DOW. These suspensions are stabilised by surface charges built up by dissociation of protons from the surface. To effectively remove counter-ions other than the dissociated protons, a mixed-bed ion-exchange resin was added to the suspension. Within a few days the repulsive interaction leads to a liquid-like structure factor $S(k)$ (figure 1) (Brown *et al* 1975). The peak position k_{max} in $S(k)$ is proportional to the cubic root of the concentration, as is expected by simple arguments (figure 2). The product $\rho^{-1/3}k_{max}/2\pi$ shows a dependence on particle size. The values are $\rho^{-1/3}k_{max} = 1{\cdot}31 \pm 0{\cdot}02$ for the particles with $0{\cdot}045$ μ radius and $\rho^{-1/3}k_{max}/2\pi = 1{\cdot}49 \pm 0{\cdot}04$ for the particles with $0{\cdot}055$ μ radius. For particles with radius $0{\cdot}025$ μ it was given by Brown *et*

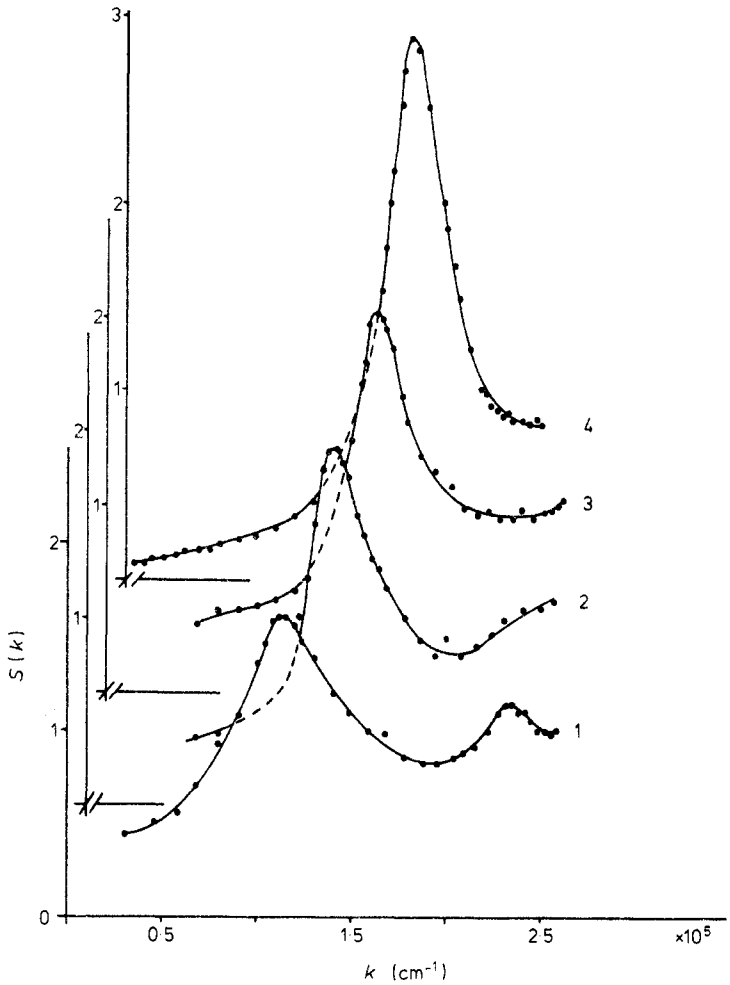

Figure 1. Static structure factors $S(k)$ for different concentrations of particles with radius of $0{\cdot}045$ μ measured with $\lambda = 6328$ Å. Concentrations (10^{12} ml^{-1}): 1, 2·53; 2, 5·06; 3, 7·59; 4, 12·65.

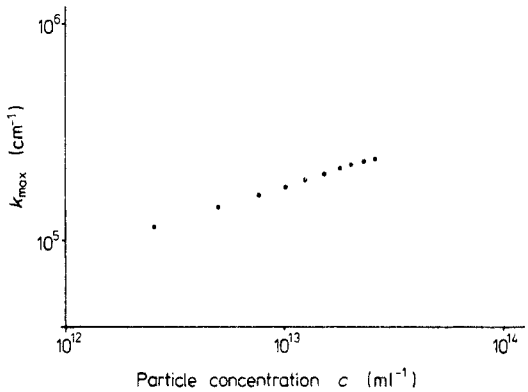

Figure 2. Dependence of the maximum of $S(k)$, k_{max}, on particle concentration. The three highest concentrations shown exhibit crystalline-like order.

al (1975) to be $\rho^{-1/3}k_{max}/2\pi = 1{\cdot}20 \pm 0{\cdot}02$. All concentrations stated are calculated from the dilution factor and the concentrations for the original solutions given by the manufacturer.

From the measured pH of the solution a charge of $1100 \pm 150\,e^-$ is calculated, assuming that all protons measured are due to the latex spheres. It should be mentioned, however, that the ordinary Debye–Hückel approximation breaks down for these macro-ions and some effective charge of about $100\,e^-$ has to be assumed (Hastings 1978).

The sample cells used are cylindrical quartz tubes with 6 mm internal diameter. They were surrounded by glycerine which acts as an index matching system and a temperature stabilised bath. The temperature used was 25 °C ± 0·5 °C.

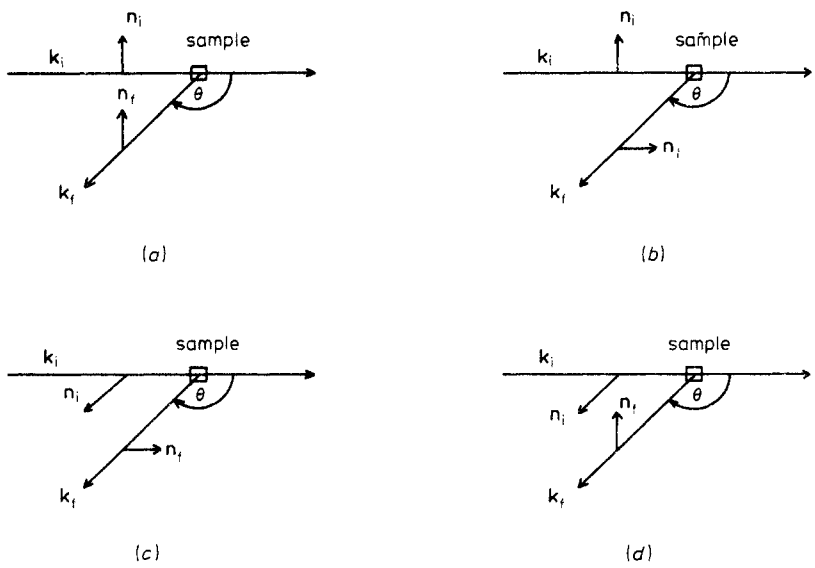

Figure 3. Definition of scattering geometries. The wavevector and polarisation vector of incoming and scattered light are denoted by $\boldsymbol{k}_i$, $\boldsymbol{n}_i$ and $\boldsymbol{k}_f$, $\boldsymbol{n}_f$ respectively. (*a*) V–V scattering, (*b*) V–H scattering, (*c*) H–H scattering, (*d*) H–V scattering.

The scattered light is focussed onto the photocathode of an RCA photomultiplier by a 20 cm lens with 1 : 1 projection of the scattering volume. This is determined by a 30 μ pinhole positioned in front of the photocathode, and the diameter of the laser focus, which is about 250 μ. We used a HeNe laser (125 Spectra Physics) with output power of 40–60 mW. Two Glan–Tompson prisms were used to define the polarisation of the incident and scattered light. The measured extinction ratio of the prisms is better than 10^{-6}. The different scattering geometries are denoted by the orientation of polariser and analyser relative to the scattering plane (figure 3).

The unclipped intensity (homodyne) correlation function is determined by means of a 4000 channel correlator; a detailed description of which will be given elsewhere (Lehmann 1980). The measured intensity correlation functions are analysed using a multi-exponential fit program developed by Provencher (1976). This program fits a flat background and a sum of up to five discrete exponentials to the data without any free parameters. The choice of the best fit is based on a nonlinear hypothesis test, and not only on the minimum of the standard deviation. By this method, described in more detail in the original paper (Provencher 1976), the number of exponentials fitted is prevented from becoming unnecessarily large.

Although there is no physical *a priori* reason to have a sum of discrete exponentials, most of the data was approximated excellently by two or three exponentials.

3. Results and discussion

3.1. Concentration dependence

At high concentration not only double but multiple scattering events have to be considered. This may be done using the model of independent successive scattering events developed for non-interacting particles in a recent paper by Sorenson *et al* (1978). The basic assumptions of this model are:

(a) the number of scattering events a photon suffers is Poisson distributed around a mean $\bar{n}$;

(b) the linewidth of n-fold scattering is n times the linewidth of single scattering at a scattering angle of 90°.

It is shown in figure 5 that this model gives an adequate description of the first cumulant of the multiple scattering, both polarised and depolarised, although a clearly peaked $S(k)$ indicating interaction effects was present in all samples except the lowest concentration (figure 1). All data were taken at 90° scattering in H–V and H–H scattering geometry (figure 3). The latter allows us to determine the polarised component of the multiple scattering alone, since the single scattering vanishes due to the dipolar nature of the scattering process, at least for small particles where the Rayleigh–Debye approximation is valid. So we were able to analyse the multiple scattering, both polarised and depolarised, without interference from the still large single scattering. The measured ratio $R^n = I^n_{VH}/I^n_{HH}$ has the value of $0{\cdot}155 \pm 0{\cdot}03$ at the lowest concentration measured. This value agrees with the value of 0·125, predicted by numerical calculation (Sorenson 1976). The first cumulants for polarised and depolarised multiple scattering coincide at the value for double scattering $2\Gamma^1_{VV}$ (90°). At higher concentrations the ratio of depolarised and polarised multiple scattering tends to one, and there is a difference in the linewidth (measured by the first cumulant) between polarised and depolarised scattering.

To consider the multiple scattering alone, the formulae (10), (13*a*, *b*) of Sorenson (1978) for the depolarisation ratio and the linewidth have to start with $n = 2$:

$$R^n = \frac{I^n_{VH}}{I^n_{HH}} = \frac{I^n_{HV}}{I^n_{HH}} = \frac{\sum_{n=2}^{\infty}[R_n/(1+R_n)]P_n(\bar{n})}{\sum_{n=2}^{\infty}[1/(1+R_n)]P_n(\bar{n})} \tag{1}$$

$$\Gamma^n_{HH} = \Gamma^1_{VV}(90°)\frac{\sum_{n=2}^{\infty}[1/(1+R_n)]nP_n(\bar{n})}{\sum_{n=2}^{\infty}[1/(1+R_n)]P_n(\bar{n})} \tag{2}$$

$$\Gamma^n_{VH} = \Gamma^n_{HV} = \Gamma^1_{VV}(90°)\frac{\sum_{n=2}^{\infty}[R_n/(1+R_n)]nP_n(\bar{n})}{\sum_{n=2}^{\infty}[R_n/(1+R_n)]P_n(\bar{n})}. \tag{3}$$

The notations are as follows. The superscript n or 1 denotes multiple and single scattering respectively, the subscripts H and V denote the scattering geometry depicted in figure 3 and $P_n(\bar{n})$ is the Poisson weight. Note that R^n and R_n are different quantities; the former denotes the polarisation ratio for the multiple scattering light as measured, whereas R_n denotes the depolarisation ratio for the n-fold scattering light with the number n of scattering events fixed. These formulae would describe the measured quantities if the depolarisation ratios R_n for an n-fold scattering process were known exactly. Only the value for double scattering has been calculated (Sorenson 1976) and experimentally verified by this work, and there is a calculated value for threefold scattering of $R_3 = 0{\cdot}26$ (Sorenson 1978). An estimate of the higher depolarisation ratios may be obtained from the following arguments. The singly scattered intensity I_1 is totally polarised and the total doubly scattered intensity $I_2 = \alpha I_1$ is split as

$$I_2^{\parallel} = \tfrac{8}{9}\alpha I_1 \qquad \text{and} \qquad I_2^{\perp} = \tfrac{1}{9}\alpha I_1. \tag{4}$$

Assuming the same splittings for the next (third) scattering event yields

$$I_3^{\parallel} = \tfrac{8}{9}\alpha I_2^{\parallel} + \tfrac{1}{9}\alpha I_2^{\perp} = \tfrac{65}{81}\alpha^2 I_1, \tag{5}$$

$$I_3^{\perp} = \tfrac{8}{9}\alpha I_2^{\perp} + \tfrac{1}{9}\alpha I_2^{\parallel} = \tfrac{16}{81}\alpha^2 I_1. \tag{6}$$

From this consideration a depolarisation ratio $R_3 = 0{\cdot}246$ is obtained which is in good agreement with the value of 0·26. This encourages us to proceed further in the same fashion. The results are listed in table 1.

Table 1. The depolarisation ratios of the n-fold scattering process.

n	R_n
2	0·125
3	0·246
4	0·464
5	0·764
6	0·965
≥7	1·0

Assuming these values for the R_n, we calculated from equations (1), (2) and (3) the cumulants and depolarisation ratios as a function of $\bar{n}$ (figure 4).

These curves are compared with the experiment in figure 5, where it is assumed that the mean number of scattering events is proportional to the particle density according to

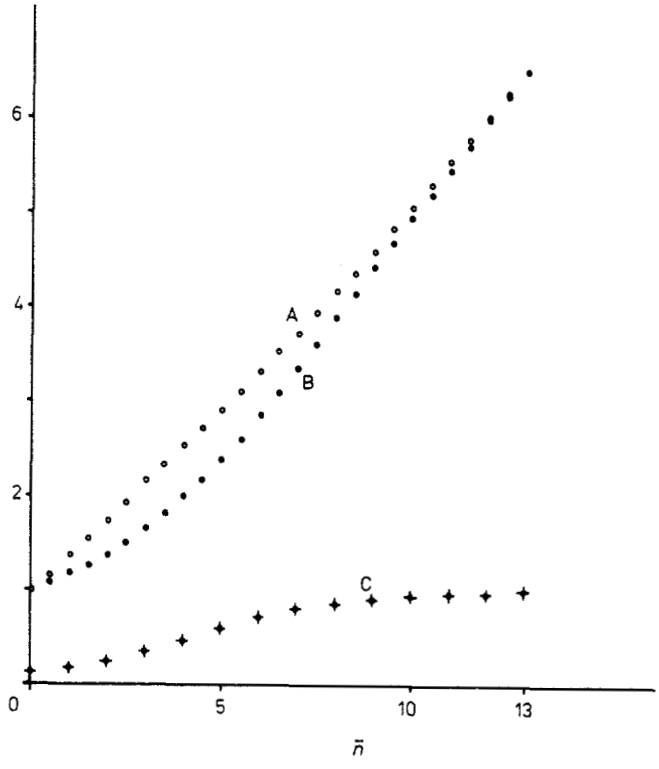

Figure 4. Cumulants Γ^n_{HH} and Γ^n_{VH} and depolarisation ratio R^n from the model of independent scattering events over the mean number of scattering events $\bar{n}$. (A) ○ $\Gamma^n_{VH}/2\Gamma'_{VV}$ (90°), (B) ● $\Gamma^n_{HH}/2\Gamma'_{VV}$ (90°), (C) ◆ $R^n = I^n_{VH}/I^n_{HH}$.

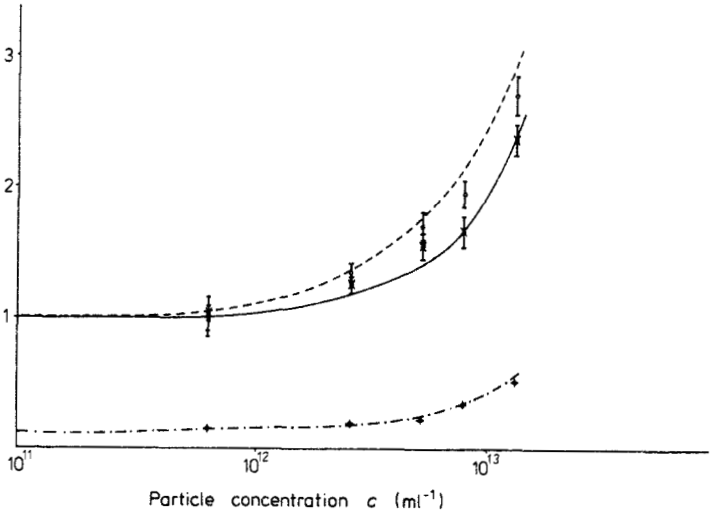

Figure 5. Concentration dependence of the multiple scattering. Shown are the first cumulants of the depolarised scattering Γ^n_{HV} and the polarised scattering Γ^n_{HH}, together with the polarisation ratio R^n. Theoretical curves are from the model of independent scattering events with $\bar{n} = c \times 0{\cdot}4 \times 10^{-12}$ cm^3. ⧖ $\Gamma^n_{HH}/2\Gamma^1_{VV}$ (90°), —— theory; ⧖ $\Gamma^n_{HV}/2\Gamma^1_{VV}$ (90°), – – – theory; ● $R^n = I^n_{HV}/I^n_{HH}$, –·–·– theory.

$\bar{n} = C \times 0{\cdot}4 \times 10^{-12}$ cm^3. As may be seen from table 2, the agreement between experiment and theory is even better if one determines the number of scattering events independently for each sample from the measured R_n. The dependence of $\bar{n}$ on concentration is then not exactly linear, but decreases at high concentrations. This might be an effect of the partially ordered state due to the interactions. The mean value of $\bar{n} = C \times 0{\cdot}4 \times 10^{-12}$ cm^3, however, which was used to calculate the theoretical lines in figure 5, gives a reasonable description too. This value moreover is in qualitative agreement with the value obtained by Rayleigh–Debye theory. From this theory a cross section of $0{\cdot}35 \times 10^{-12}$ cm^2 is obtained. This yields a mean free path of the photon of approximately 1 cm within the cell, which is of the order of the scattering cell diameter (0·6 cm).

Table 2. The transmission Tr and depolarisation ratio R^n of multiple scattering, the mean number of scattering events $\bar{n}$ determined from R^n, and the first cumulants of polarised and depolarised multiple scattering as a function of particle concentration c.

c(ml^{-1})	Tr	$R^n = I^n_{HV}/I^n_{HH}\bar{n}$	$\bar{n}$
$0{\cdot}63 \times 10^{12}$	0·89	0·155 ± 0·03	0·6 ± 0·1
$2{\cdot}5 \times 10^{12}$	0·65	0·195 ± 0·01	1·4 ± 0·1
$5{\cdot}1 \times 10^{12}$	0·50	0·254	2·0
$7{\cdot}6 \times 10^{12}$	0·40	0·343	2·8
$12{\cdot}7 \times 10^{12}$	0·21	0·513	4·1

c(ml^{-1})	$\Gamma^n_{HH}/2\Gamma^1_{VV}$ (90°) experimental	$\Gamma^n_{HH}/2\Gamma^1_{VV}$ (90°) calculated	$\Gamma^n_{HV}/2\Gamma^1_{VV}$ (90°) experimental	$\Gamma^n_{HV}/2\Gamma^1_{VV}$ (90°) calculated
$0{\cdot}63 \times 10^{12}$	1·02 ● 0·12	1·10 ± 0·15	0·99 ± 0·10	1·2 ± 0·15
$2{\cdot}5 \times 10^{12}$	1·26 ± 0·06	1·20 ± 0·05	1·35 ± 0·07	1·38 ± 0·05
$5{\cdot}1 \times 10^{12}$	1·52 ± 0·10	1·45	1·70 ± 0·10	1·72
$7{\cdot}6 \times 10^{12}$	1·66 ± 0·08	1·63	1·96 ± 0·08	2·05
$12{\cdot}7 \times 10^{12}$	2·38 ± 0·09	2·31	2·72 ± 0·10	2·70

We want to conclude this section with some remarks concerning non-interacting particles. It was shown by Sorenson *et al* (1978) that the model gives a good description in the case of non-interacting particles. We have shown here that the model works surprisingly well even in the presence of interactions. To elucidate this we have also done some measurements at a temperature of 51 °C. At this temperature the peak in $S(k)$ becomes considerably weaker, indicating that the interaction effects are becoming less important at these temperatures. We will not discuss these experiments in detail, but simply state the fact that the depolarisation ratios R^n increase by about 10% at the same concentration when the interactions are switched off by the higher temperature. This behaviour, together with table 2, leads to the conclusion that the mean number of scattering events $\bar{n}$ which is extracted from R^n plays the role of a free parameter and has to be adjusted for every particular experiment made. The values for the cumulants calculated from this $\bar{n}$ then give a reasonable estimate of the cumulants expected for the multiple scattering, both polarised and depolarised.

It should be further noted that the cumulants for depolarised and polarised multiple scattering light do not differ seriously, since the maximum deviation is 24% in the calculations. This difference seems to be even less if one looks at the experiments.

3.2. Angular dependence

Up to now the presence of interaction has been totally neglected in our calculations and it has been shown that the model of independent scattering events gives a very good description of the cumulants at 90°. We are now going to look a little closer at the depolarised scattering obtained from two samples. Sample I consists of $3{\cdot}1\times10^{12}$ particles of $0{\cdot}055\,\mu$ radius per millilitre; sample II, the sample with the highest concentration discussed in § 3.1 has $12{\cdot}7\times10^{12}$ particles of $0{\cdot}045\,\mu$ radius per millilitre. The samples were chosen because they show their maximum of $S(k)$ in the vicinity of 90° for the HeNe laser-wavelength (figure 6), where the biggest effect on the angular dependence is expected (Böheim *et al* 1979). Note that the peak at sample I is rather broad compared with e.g. sample II, indicating that not all counter-ions have been removed. This tends to move $k_{\max}$ to larger k-values (see Brown *et al* 1975). Thus, for this particular sample $k_{\max}\rho^{-1/3}/2\pi = 1{\cdot}49$ does not hold. It is possible that to some extent coagulation has occured. However, since we are only concerned with a comparison of static and dynamical measurements, this does not affect the conclusions we want to draw from the experiments.

For a theoretical description of the multiple scattering a numerical calculation is needed, and to make things easy and transparent we have exploited the model of independent scattering events a little more by performing a Monte Carlo simulation of multiple scattering. The simulation was based on the same principles as the model of independent scattering events, namely:

(a) every scattering process gives rise to a scattered intensity

$$I(k') = S(k')\sin^2\theta'/I_0,$$

where k' is the intermediate scattering vector, θ' is the angle between the actual scattering plane and the direction of the outgoing wave and $I_0 = \int S(k')\sin^2\theta'\,\mathrm{d}\Omega$ is a normalisation constant which sets the total scattered intensity to unity;

(b) with every scattering process a term $\Gamma(k') = D_0 k'^2/S(k')$ is added to the total width of the spectrum, which is the appropriate expression in the presence of interaction (Pusey 1975).

Assumption (a) is equivalent to the far-field approximation for the dipole radiation. Assumption (b) is a rather crude approximation, which firstly retains only high-order intensity correlations which are factorisable and secondly neglects all deviations from single exponential behaviour in the single scattering correlation function (Pusey 1978, Grüner and Lehmann 1979).

For fixed initial and final wavevectors k_i and k_f the following quantities are calculated for an n-fold scattering process:

(a) the polarised intensity

$$I^n_{HH} = I^n_{VV}(\theta) = \left\langle \left(\prod_{i=1}^{n} I(k'_i) \right)_{VV} \right\rangle; \tag{7}$$

(b) the depolarised intensity

$$I^n_{VH}(\theta) = \left\langle \left(\prod_{i=1}^{n} I(k'_i) \right)_{VH} \right\rangle; \tag{8}$$

(c) the cumulant for polarised scattering

$$\Gamma^n_{HH}(\theta) = \left\langle \left(\prod_{i=1}^{n} I(k'_i) \right)_{HH} \sum_{i=1}^{n} \Gamma(k'_i) \right\rangle \Big/ I^n_{HH}(\theta); \tag{9}$$

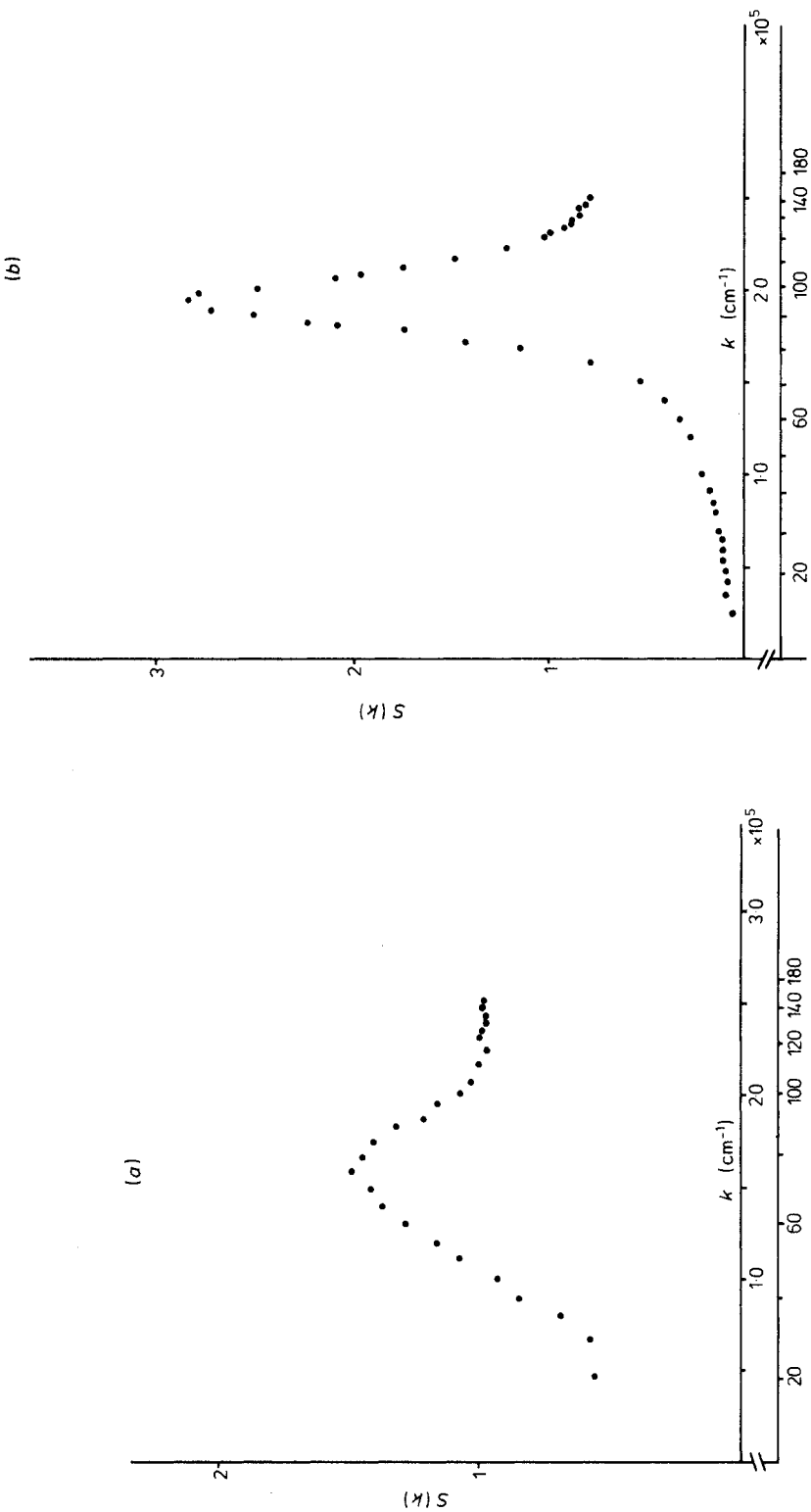

Figure 6. Static structure factors $S(k)$. (*a*) Sample I, concentration $3{\cdot}1\times10^{12}$ particles ml^{-1}, radius 0·055 μ. (*b*) Sample II, concentration $12{\cdot}7\times10^{12}$ particles ml^{-1}, radius 0·045 μ (same as figure 1).

(d) the cumulant for depolarised scattering

$$\Gamma^n_{VH}(\theta) = \left\langle \left(\prod_{i=1}^{n} I(k_i') \right)_{VH} \sum_{i=1} \Gamma(k_i') \right\rangle \Big/ I^n_{VH}(\theta). \tag{10}$$

The parallel and perpendicular polarisations refer to the original scattering plane and are easily calculated from the intermediate polarisation vectors involved. The angular brackets indicate an average over randomly chosen intermediate scattering vectors equally distributed over the surface of a sphere, which is the appropriate distribution for a spherical scattering volume. For double scattering this procedure is equivalent to a Monte Carlo integration of the formulae used by Sorenson *et al* (1976) and Böheim *et al* (1979). Ten thousand scattering processes were averaged, which gave an accuracy better than 1% in the double scattering without interaction compared with the exact results of Sorenson *et al* (1976). We have also obtained the value 0·26 (independent of angle) for the depolarisation ratio of triple scattering without interaction given by Sorenson (1978).

With this model we are now able to calculate the angular dependence of the multiple scattering and compare it with our experimental results. The static structure factors measured by the intensity of single scattering are given in figure 6(*a*) for sample I and figure 4(*b*) for sample II. For the latter it was necessary to correct for the multiple scattering. This was done by the following method, which is applicable for small spherical scatterers where it is possible to measure the depolarisation ratio for multiple scattering, $R^n = I^n_{VH}/I^n_{HH}$. Under the reasonable assumption that the depolarisation ratio R^n is independent of the scattering angle, an assumption which is supported by calculating R^n according to equations (7) and (8), the multiple scattering may be measured separately in the VH-polarisation. The static structure factor is then given as a difference of two readily measured quantities, the intensity in VV-polarisation I^{meas}_{VV} and the intensity in VH-polarisation I^{meas}_{VH}

$$S(k) \propto I^1_{VV}(\theta) = I^{meas}_{VV}(\theta) - \frac{1}{R^n} I^{meas}_{VH}(\theta). \tag{11}$$

This correction was especially necessary at small scattering angles, where the single and the multiple scattering were of the same order of magnitude. The result of the fit to the intensity correlation for the depolarised light is given in figure 7 for sample I, together with the result of the calculation for double scattering (dashed line). The calculated results are in qualitative agreement with the calculations of the double scattering performed by Böheim *et al* (1979). The differences in the numerical values between the two results are only due to the different static structure factors. The experimentally determined times of the short component are in good agreement with the calculation. Triple scattering would give decay times of about two-thirds of the times for double scattering, which would lie below the experimental points. Thus it is not considered here although it should be present. However, there is a second component present. It is somewhat surprising that two decay times were always found by the fit, since a broad distribution of decay times is expected, which in the case of non-interacting particles lie within the bounds

$$[4D_0k_0^2(1+\cos\tfrac{1}{2}\theta)]^{-1} < \tau < [4D_0k_0^2(1-\cos\tfrac{1}{2}\theta)]^{-1} \tag{12}$$

where k_0 is the wavevector of the incident beam (Böheim *et al* 1979). These bounds are given by the full lines in figure 5 and it can be seen that the long-time decay constant

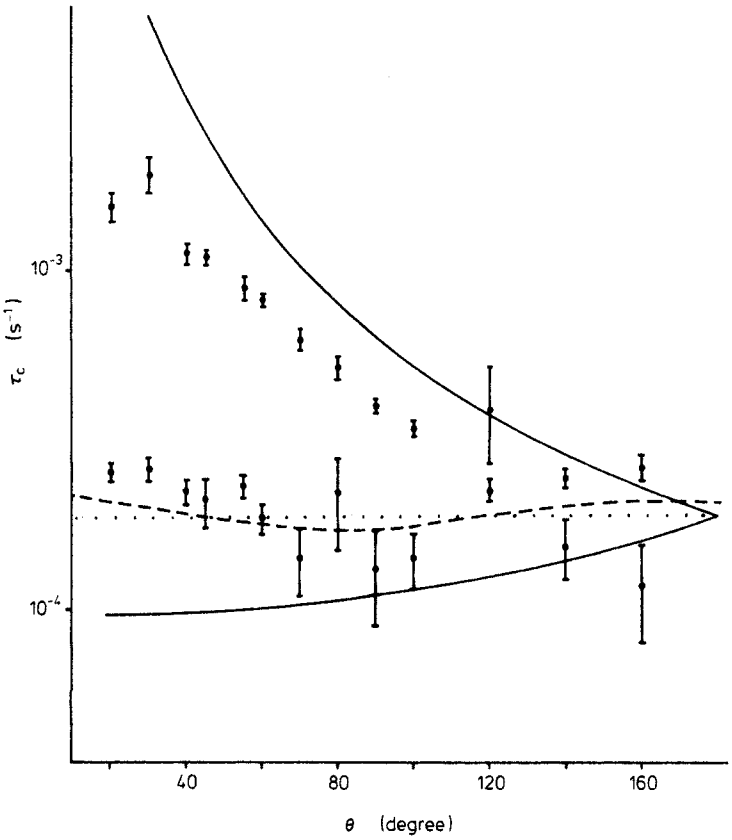

Figure 7. Depolarised scattering from sample I. Shown are the decay times obtained from the fit to the intensity-correlation function and the calculated cumulant for double scattering (------), together with the short- and long-time limits (——). The double scattering without interaction would follow the dotted line.

follows approximately the upper bound, although no interaction effects are included in this bound. It is also possible that the main contributions to this long times arise from the long-time tail, which is present in the single scattering due to the particle interactions (Pusey 1978, Grüner and Lehmann 1979). Even the effect of sample contamination cannot be excluded from this particular sample. It should be noted that the experimental cumulant lies above the calculated values due to this long-time tail, and the agreement is only reasonable for the short-time component of the fit.

This behaviour is even more pronounced in sample II. The fit results are displayed in figure 8 together with the calculated cumulants for double, triple and fourfold scattering. Since the correlation functions are non-exponential, in most cases three exponentials were needed to fit the data. It should be noted that the individual components of the different multiple scattering processes are not resolved by the fit and that the distribution of decay times is broader than that given by the calculation. Again, a long-time tail is present, especially in the forward direction. On the other hand, a very short time is present at larger scattering angles. The time involved would correspond to a tenfold-scattering-process (arrows), a process which is very unlikely even at these high concentrations.

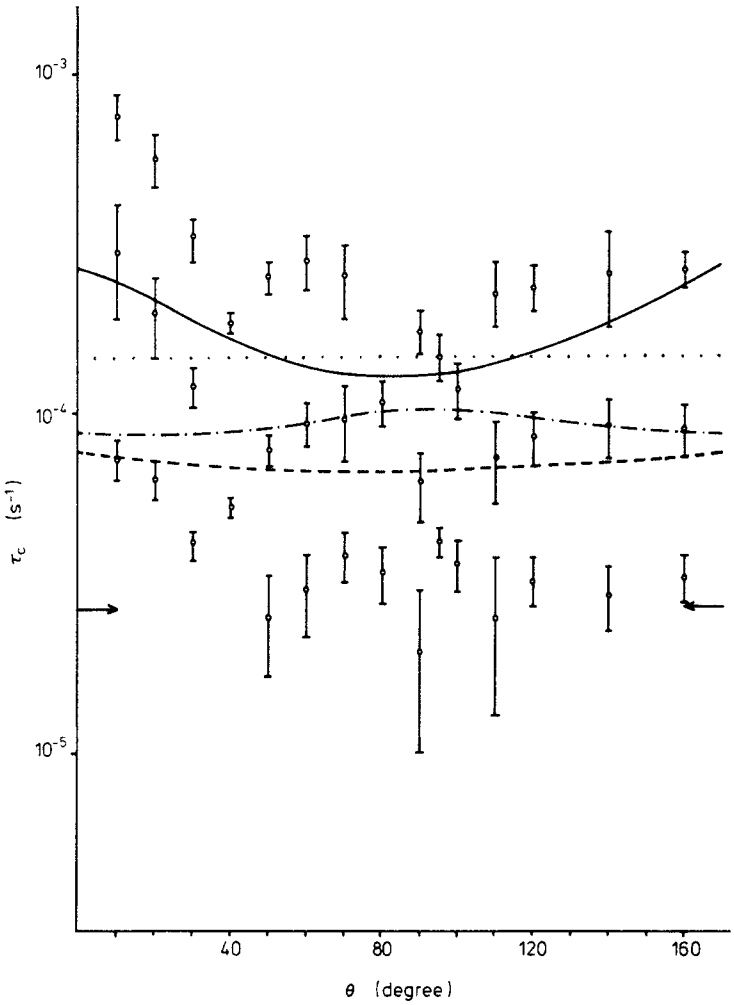

Figure 8. Depolarised scattering from sample II. The experimental points are from the fit to the intensity correlation. Also shown are the calculation for double scattering (——), triple scattering (–·–) and fourfold scattering (------). The arrows indicate the time for a tenfold scattering process, and the double scattering without interaction is indicated by the dotted line.

These discrepancies show up more clearly if one looks at the first cumulants (figure 9), which are weighted averages of all exponentials found. Here the experimental values are compared with calculated averaged cumulants weighted with the Poisson distribution $P_n(\bar{n})$ of the number of scattering events:

$$\Gamma^n_{\mathrm{VH}}(\theta, \bar{n}) = \sum_{n=1}^{12} I^n_{\mathrm{VH}}(\theta)\Gamma^n_{\mathrm{VH}}(\theta)P_n(\bar{n}) \Big/ \sum_{n=1}^{12} I^n_{\mathrm{VH}}(\theta)P_n(\bar{n}). \tag{13}$$

The summation was performed up to twelve-fold scattering; thus more than 99% of all possible scattering events are covered. The results are shown for $\bar{n} = 2{\cdot}5$, 3, $3{\cdot}5$ and 4. The best choice seems to be a value of $3{\cdot}5$, but there are considerable deviations, especially at small scattering angles. Note that the cumulants of HV and VH geometry

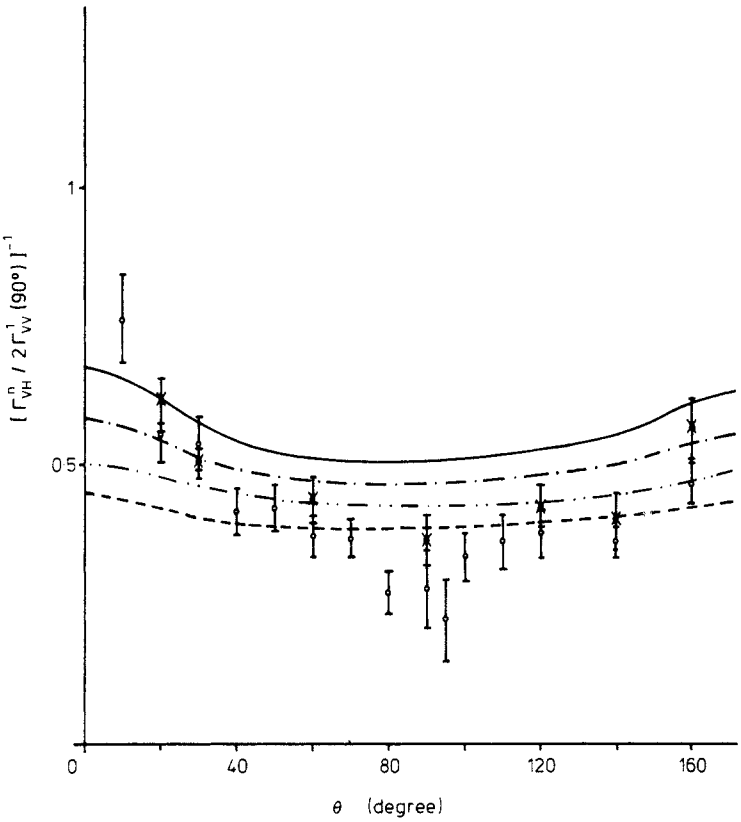

Figure 9. The cumulant of the depolarised scattering from sample II. Circles are VH-, full points are HV-Geometry. The curves are results of the calculation for mean numbers of scattering events of $\bar{n} = 2{\cdot}5$, (——); $\bar{n} = 3$, (– · – ·); $\bar{n} = 3{\cdot}5$, (– · · –); $\bar{n} = 4$, (------). ○ V–H scattering, ⧖ H–V scattering.

agree within experimental error. This proves the assumption made, that there is no difference between these geometries.

All the deviations between experiment and model calculations indicate that the model of independent scattering events is no longer a good description if one wants to look at the finer details like angular dependence, although the coarse features like concentration dependence are described very well. It is certainly necessary to have a better description of multiple scattering, taking into account the effects of higher-order correlation functions, non-single-exponential behaviour of the single scattering, and the exact dipole propagator of light, since the far-field assumption seems not to be justified when the mean distance between particles is of the order of the wavelength of light.

4. Conclusions

The purpose of this section is to compile the results which are applicable to highly concentrated systems of small spherical Brownian particles. From these conclusions we give a guide to how a correction for multiple scattering may be possible. The first result

of our investigation is that the model of independent scattering events gives a good description of the effects of multiple scattering if one does not go too far into the details. The second result is that, except at low scattering angles, the decay times emerging from multiple scattering are of the order of the single scattering at 180°, as it is the case without interactions present. Thus, only the short-time behaviour of the intensity correlation function in VV-geometry is affected. The third result, which was checked at a scattering angle of 90°, is that the differences between decay times of depolarised and polarised multiple scattering are not large. So we propose the following method to account for the multiple scattering.

(1) To get a feeling for the order of magnitude of multiple scattering, one should measure the intensity of multiply scattered light in HV- and HH-geometry at scattering angle of 90°. From the depolarisation ratio $R^n = I^n_{HV}/I^n_{HH}$ one may estimate the mean number of scattering events $\bar{n}$ and the polarised intensity of the multiply scattered light.

(2) If the amount of multiply scattered light determined in this way is not negligible, one has to measure the depolarised intensity and correlation function for the scattering angles needed. By analysing the polarised and depolarised intensity correlation function with a multiexponential fit, one is able to identify the multiply scattered components, allowing for deviations between parallel polarised and depolarised multiple scattering times estimated from the model of independent scattering events (figure 5). It is then straightforward to subtract the undesired components from the correlation function. We have never found, using this method, any indication for a cross term between multiply and singly scattered light in agreement with theoretical predictions (Bøe and Sikkeland 1977).

(3) A cross check is to compare the first cumulant obtained in this manner with the theoretical value $D_0k^2/S(k)$, where $S(k)$ is the static structure factor corrected for multiple scattering as described in the text.

We want to demonstrate the procedure by an example. We chose rather arbitrarily a measurement at the peak of $S(k)$ in the sample II (figure 6(*b*)). We measured the intensity correlation function in VV- and VH-geometry. The results of the fit procedure are given in table 3.

The multiply scattered components are readily identified by their decay constants, which are smaller in the polarised correlation function as expected, but agree almost within experimental error. There is however a mismatch in the relative amplitudes. Since the measured $S(k)$ is 2·8, and from a measurement at low concentration $2D_0k^2$ is determined to be $3{\cdot}67\times10^3\ s^{-1}$, the first component in table 3 is totally due to multiple

Table 3. Fit results for the intensity correlation function in VV- and VH-geometry for $\theta = 95°$ ($k = k_{max}$) for a sample of $12{\cdot}7\times10^{12}$ particles ml^{-1} with radius 0·045 μ. The amplitudes are normalised independently to 1.

Intensity correlation function in VV-geometry		Intensity correlation function in VH-geometry	
Relative amplitude α	Decay constant Γ $[s^{-1}]$	Relative amplitude α	Decay constant Γ $[s^{-1}]$
0·18 ± 0·05	$(1{\cdot}52\pm0{\cdot}34)\times10^4$	0·54 ± 0·07	$(2{\cdot}38\pm0{\cdot}24)\times10^4$
0·28 ± 0·09	$(4{\cdot}43\pm1{\cdot}54)\times10^3$	0·46 ± 0·03	$(6{\cdot}80\pm1{\cdot}15)\times10^3$
0·22 ± 0·10	$(1{\cdot}77\pm0{\cdot}65)\times10^3$		
0·32 ± 0·04	$(6{\cdot}14\pm0{\cdot}30)\times10^2$		

scattering. Therefore we subtract this component and a fraction of 0·15 of the second component, so we are left with the components of the intensity correlation listed in table 4.

Table 4. Remaining components of the intensity correlation function after correction for multiple scattering.

Relative amplitude	Decay constant Γ [s^{-1}]
0·13	$(4{\cdot}43 \pm 1{\cdot}54) \times 10^3$
0·22	$(1{\cdot}77 \pm 0{\cdot}65) \times 10^3$
0·32	$(6{\cdot}14 \pm 0{\cdot}30) \times 10^2$

We calculate the first cumulant according to the formula

$$\Gamma_{cu} = \left(\sum_i \alpha_i \Gamma_i\right) \Big/ \sum_i \alpha_i$$

where α_i is the amplitude of the ith component and the summation runs over all components under consideration. The uncorrected correlation function yields a first cumulant of $4{\cdot}56 \times 10^3$ s^{-1}, which is $2{\cdot}48 \times D_0 k^2$ and would correspond to $S(k)$ of about 0·8. The corrected correlation function yields a first cumulant of $1{\cdot}496 \times 10^3$ s^{-1}, which is $0{\cdot}411 \times D_0 k^2$ and corresponds to $S(k)$ of about 2·4, which should be compared to the measured value of 2·8. Within the errors given by the fit it is also possible to discard the second component of the VV-correlation function as being entirely due to multiple scattering. In this case a cumulant of $1{\cdot}08 \times 10^3$ s^{-1} is obtained, which yields $S(k) = 3{\cdot}4$.

In our opinion, the example given above shows very markedly the benefits and limitations of the method. On one hand no correction leads to disastrous wrong cumulants, on the other hand one has to make very accurate measurements to make good corrections for multiple scattering when there is a chance of having decay constants in single and multiple scattering which are not well separated. We would like to point out the fact that the procedure is much more convenient in less concentrated samples where a smaller number of decay constants is involved.

There are several uncertainties involved with this procedure, since the angular dependence of the polarised component of multiple scattering is not accessible in the whole range of angles and there is no satisfactory theory for the angular dependence of multiple scattering. However, we think that assuming the same depolarisation ratios R_n and differences in the characteristic times between polarised and depolarised components over the whole angle is not an unreasonable assumption, and we have not found any contradiction to this assumption up to now. Moreover we feel that our procedure is at present the best attempt to account for multiple scattering.

Acknowledgments

The authors wish to thank Professor Weber for his encouragement and support, and Dr Heß and Professor Klein, Konstanz, and Dr Fijnaut, Utrecht, for helpful discussions. The numerical calculations were performed on a TR 440 computer at 'Rechenzentrum der Universität Konstanz'.

References

Berne B and Pecora R 1976 *Dynamic Light Scattering* (New York: Wiley)
Bøe A and Sikkeland I 1977 *Phys. Rev.* A **16** 2105
Böheim J, Hess W and Klein R 1979 *Z. Phys.* B **32** 237
Brown J C, Pusey P N, Goodwin J N and Ottewill R H 1975 *Z. Phys.* A **8** 664
Grüner F and Lehmann W 1979 *J. Phys. A: Math. Gen.* **12** L303
Hastings R 1978 *J. Chem. Phys.* **68** 675
Lehmann W 1980 submitted for publication
Provencher S W 1976 *J. Chem. Phys.* **64** 2772
Pusey P N 1975 *J. Phys. A: Math. Gen.* **9** 1433
—— 1978 *J. Phys. A: Math. Gen.* **11** 119
Sorensen G M, Mockler R C and O'Sullivan W J 1976 *Phys. Rev.* A **14** 1520
—— 1978 *Phys. Rev.* A **17** 2030